The effect of nanocrystalline magnetite size on arsenic removal

Available online at www.sciencedirect.com
ScienceDirect
Science and Technology of Advanced Materials 8 (2007) 71–75
SCIENCE AND TECHNOLOGY OF ADVANCED MATERIALS
www.elsevier.com/locate/stam

The effect of nanocrystalline magnetite size on arsenic removal

J.T. Mayo[a], C. Yavuz[a], S. Yean[b], L. Cong[b], H. Shipley[b], W. Yu[a], J. Falkner[a], A. Kan[b], M. Tomson[b], V.L. Colvin[a,*]

[a]*Department of Chemistry, Rice University, 6100 Main Street, Houston, TX 77005, USA*
[b]*Department of Civil and Environmental Engineering, Rice University, 6100 Main Street, Houston, TX 77005, USA*

Received 25 July 2006; received in revised form 7 October 2006; accepted 11 October 2006
Available online 18 December 2006

Abstract

Higher environmental standards have made the removal of arsenic from water an important problem for environmental engineering. Iron oxide is a particularly interesting sorbent to consider for this application. Its magnetic properties allow relatively routine dispersal and recovery of the adsorbent into and from groundwater or industrial processing facilities; in addition, iron oxide has strong and specific interactions with both As(III) and As(V). Finally, this material can be produced with nanoscale dimensions, which enhance both its capacity and removal. The objective of this study is to evaluate the potential arsenic adsorption by nanoscale iron oxides, specifically magnetite (Fe_3O_4) nanoparticles. We focus on the effect of Fe_3O_4 particle size on the adsorption and desorption behavior of As(III) and As(V). The results show that the nanoparticle size has a dramatic effect on the adsorption and desorption of arsenic. As particle size is decreased from 300 to 12 nm the adsorption capacities for both As(III) and As(V) increase nearly 200 times. Interestingly, such an increase is more than expected from simple considerations of surface area and suggests that nanoscale iron oxide materials sorb arsenic through different means than bulk systems. The desorption process, however, exhibits some hysteresis with the effect becoming more pronounced with small nanoparticles. This hysteresis most likely results from a higher arsenic affinity for Fe_3O_4 nanoparticles. This work suggests that Fe_3O_4 nanocrystals and magnetic separations offer a promising method for arsenic removal.

Keywords: Arsenic removal; Magnetic separation; Magnetite; Nanoparticles; Sorption

1. Introduction

Arsenic(As)-contaminated drinking water is a major problem around the world. Countries such as Bangladesh, India, Vietnam, Mexico, Argentina, Chile, Hungary, Romania, and the United States face significant challenges in meeting the newly lowered standards for As in drinking water [1]. Several methods of As removal are already available including precipitation, adsorption, ion exchange, solvent extraction, nanofiltration, foam flotation, and biological sequestration [2]. However, as recently noted these technologies cannot perform well in actual field trials, and improved materials and systems are needed [3]. In particular, sorbents must be able to achieve a low As level in drinking water for geographical areas with high As concentrations. Many papers have been published demonstrating that bulk iron oxides have a high affinity for the adsorption of arsenite and arsenate [1,4,5]. As can form inner sphere monodentate or bidentate–binuclear complexes with iron oxides. Extended X-ray absorption fine structure spectroscopy has provided direct evidence for inner sphere adsorption of arsenite and arsenate on iron oxides [6–8].

There are many practical and theoretical advantages of using nanocrystals for separations. In one case, the sorption of As onto nanostructured iron films was efficient and of high capacity [9]. However, such solid systems can have slow mass transport and complex recycling processes. A better option is to use dispersed nanoparticles, which are homogeneously distributed in solution; such a system has favorable mass transport to surfaces and can permit magnetic capture of depleted materials [10]. In addition,

*Corresponding author: Tel.: +1 713 348 5741; fax: +1 713 348 2578.
E-mail address: colvin@rice.edu (V.L. Colvin).

1468-6996/$ - see front matter © 2006 NIMS and Elsevier Ltd. All rights reserved.
doi:10.1016/j.stam.2006.10.005

dispersed sorbents avoid many of the classical problems of filtration related to occluding and fouling of packed columns and membranes. Specifically for this work, magnetic separations are also possible for nanoscale materials. In one case, magnetite (Fe_3O_4) nanoparticles in biological separations were highly efficient because of the extremely small particle size and a large surface area without a high-mass-transfer resistance [11].

In this work, we show the effect of Fe_3O_4 particle size on the adsorption and desorption behaviors of arsenite (As_2O_5) and arsenate (As_2O_3). Laboratory-prepared near-monodisperse Fe_3O_4 nanocrystals are compared with commercially available Fe_3O_4 nanoparticles to determine the As removal efficiency from water [12].

2. Experimental

2.1. Materials

FeO(OH) from Aldrich (iron(III) oxide, hydrated; catalyst grade, 30–50 mesh; cat. #371254) was ground to 100–150 mesh. Oleic acid (90% technical grade) and 1-octadecene (90% technical grade) were purchased from Aldrich. Hexanes (certified ACS grade) were purchased from Fisher Scientific. A 20 nm Fe_3O_4 sample was purchased from ready advanced materials, and a 300 nm Fe_3O_4 sample was purchased from Sigma-Aldrich. The As(V) and the As(III) stock solutions were prepared by dissolving the corresponding As oxides (As_2O_5 and As_2O_3) in de-ionized water with 4 g/L NaOH.

2.2. Synthesis and preparation of magnetite nanocrystals

A scalable one-pot synthesis of Fe_3O_4 nanocrystals was performed by taking a mixture of FeO(OH) (2.00 mmol), oleic acid (8.00 mmol), and 1-octadecene (20.00 mmol); and heating with stirring at 320 °C and kept at this temperature for a desired time, as seen in Yu et al. [13]. These nanocrystals were then made water-soluble by methods similar to those seen in the work performed by Landfester and coworkers [14].

2.3. Magnetic separations

Magnetic separations were performed with a high-gradient magnetic field column separator consisting of an S.G. Frantz Canister Separator (model L-1CN), which had a stainless-steel canister column (6.3, 25.4, and 222.3 mm in length, 35.5 cm^3). The stainless-steel column was packed with stainless-steel wool (~50 μm wire diameter), with a packing volume of 5% of the canister (~15 g stainless-steel wool). A magnetic field was applied, and then a sample was passed through the column. The nanoparticles were retained in the column as the solvent passed through. When the magnetic field was removed and fresh solvent passed through the column, the nanoparticles were recovered (Fig. 1).

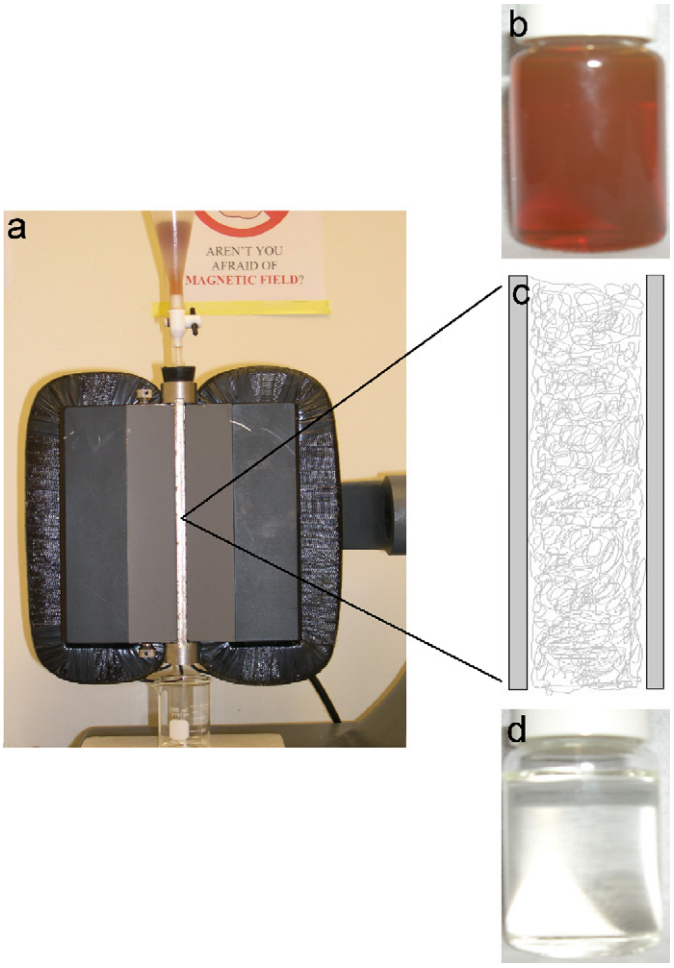

Fig. 1. Schematic of magnetic separator. A high-gradient magnetic field column separator (a) consisting of an S.G. Frantz Canister Separator (model L-1CN) was used for the magnetic separation experiments. The brown Fe_3O_4 suspension (b) was passed through a stainless-steel wool-packed column (c) within the magnetic separator. The colorless effluent (d) demonstrates the removal of magnetite.

2.4. Sorption

Sorption studies were performed on three sizes of Fe_3O_4 at As concentrations ranging from 0 to 0.45 mmol/L. The concentrations of iron as Fe_3O_4 were 2.5 and 0.1 g/L for commercially made 300 and 20 nm Fe_3O_4, respectively. The concentration of iron as Fe_3O_4 was 0.011 g/L for laboratory-prepared 12 nm Fe_3O_4 nanocrystals. Adsorption studies were conducted at pH 4.8, 6.1, and 8.0. A background electrolyte of 0.01 M $NaNO_3$ was used for the adsorption studies. 2(*N*-Morpholino)-ethanesulfonate and Tris at 0.005 M were added as buffers for 6.1 and 8.0 pH experiments, respectively. For 12 nm Fe_3O_4 nanoparticles, 0.01 M $NaNO_3$ and 0.01 M Tris buffer at pH 8 was used as an electrolyte background solution. A trace amount of HNO_3 or NaOH was used to adjust pH. The Fe_3O_4 As mixtures were equilibrated on a slowly rotating rack that tumbled end-over-end (4 rpm) for 24 h, and centrifuged at 4000 rpm for 30 min. The supernatant

solutions of the 300 and 20 nm commercially made Fe_3O_4 solutions were filtered through 0.2 μm Nalgene syringe filters (Surfactant-Free Cellulose Acetate). For the 12 nm laboratory-prepared Fe_3O_4, a magnetic field column separator was used to separate the solid from liquid phase. All experiments were performed in triplicate, and solutions analyzed for As and Fe by inductively coupled plasma-mass spectrometry (ICP-MS) (Perkin-Elmer Elan 9000) and inductively coupled plasma-optical emission spectrometry (ICP) (Perkin-Elmer Optima 4300 DV), respectively.

2.5. Desorption

Desorption studies were conducted only with the 20 and 300 nm Fe_3O_4 at pH 6.1, by adding As-free electrolyte to the As-exposed Fe_3O_4 nanoparticles which were previously used for a 24 h adsorption. Desorption experiments with 12 nm Fe_3O_4, however, were not performed because of limited samples. These samples were allowed to react for 24 h on a tumbler and centrifuged. The supernatant solution was pipetted into a syringe filter and filtered through 0.2 μm Nalgene syringe filters.

Successive desorption was done by repeating the above desorption procedures after the supernatant solution was removed. As concentrations were then measured by ICP-MS. The solid phase concentration was found from the solution phase As concentrations by assuming mass balance.

3. Results and discussion

The synthesis of Fe_3O_4 nanocrystals is successful at a variety of sizes with near-monodisperse size distributions [13]. These particles prepared in the laboratory can be easily dispersed in aqueous phase as described in the previous section. This work also uses commercially available nanoscale iron oxides. While these materials are more polydisperse, large amounts are available and the two sizes (20 and 300 nm) are readily suspended in water [12,13]. In addition to a difference in size, these commercial materials are also more aggregated in suspension than the laboratory-prepared materials. The dispersed Fe_3O_4 nanocrystals can be removed from the solution through interactions with a magnetic column. The 20 nm commercially made nanocrystals were permanently retained in the column and could not be recovered, while the laboratory-prepared nanocrystals were able to be recovered when the magnetic field was turned off (Fig. 2). Furthermore, when the magnetic field is increased, a greater percentage of nanocrystals are retained in the column (Fig. 3).

Fig. 2 shows the starting Fe_3O_4 dispersions, effluents after passage through the column at various magnetic fields, and the solutions with the recovered nanoparticles after removal of the external magnetic field. Initially, the solutions are colored due to the presence of nanoparticles (first column). When they are exposed to the magnetic column, the nanoparticles adhere to the steel wool and the

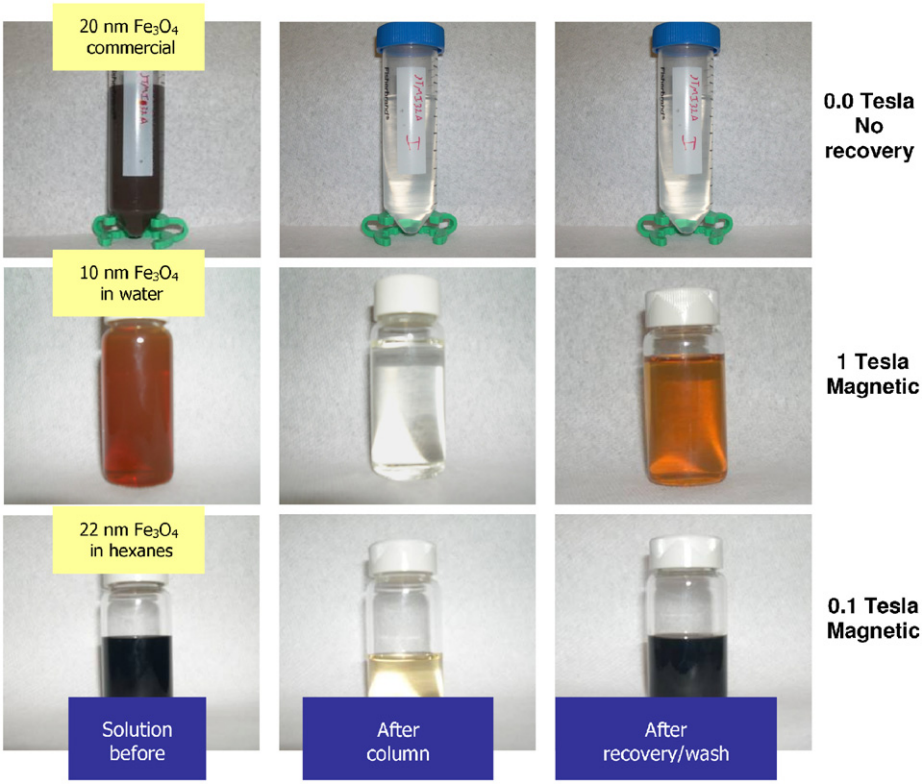

Fig. 2. Magnetic separation of nanoparticles. The top row shows 20 nm, agglomerated Fe_3O_4 in an aqueous solution and the effluent after passing through the magnetic column. The middle row shows 10 nm, laboratory-prepared Fe_3O_4 in an aqueous solution and the effluent after passing through the magnetic column. The bottom row shows 22 nm, laboratory-prepared Fe_3O_4 in a solution of hexanes and the effluent after passing through the magnetic column.

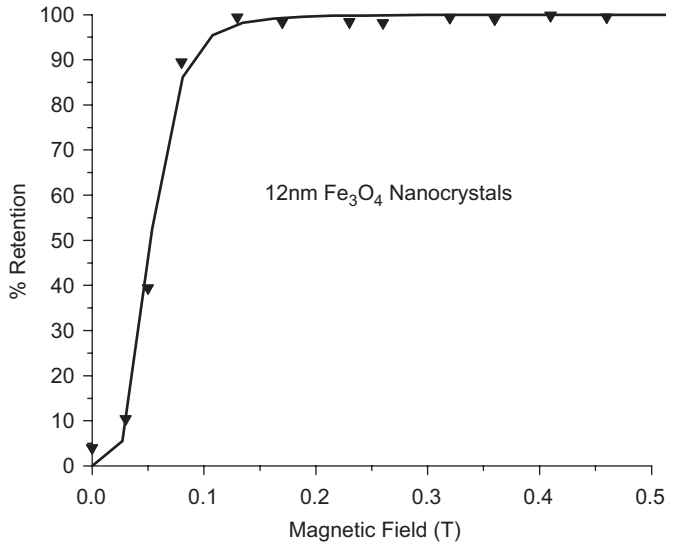

Fig. 3. Magnetic field dependence of particle retention. As the magnetic field increases, the retention of Fe_3O_4 nanocrystals increases.

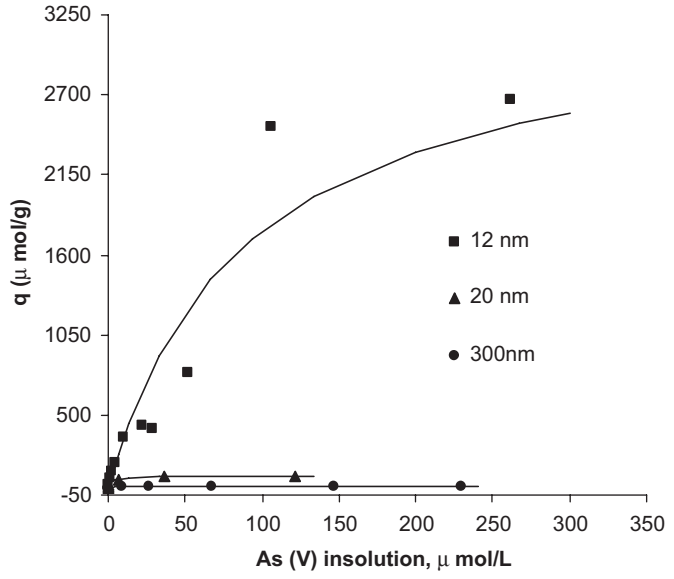

Fig. 4. Plot of As(V) adsorption on different magnetite nanoparticles (i.e., 12, 20, and 300 nm). The solid lines are drawn using Langmuir isotherm equation. All adsorption data were plotted as equilibrium adsorbed arsenic versus equilibrium arsenic in solution. In this graph, q refers to the moles of arsenic adsorbed per mass of magnetite given in units of μmol/g.

effluent at the bottom of the column is clear (second column). Finally, in some cases, the nanoparticles are recoverable once the magnetic field is removed and can be collected in a washing procedure (third column). The recovery process is effective for small nanoparticles, but not for large ones. The agglomerated, commercial nanoparticles cannot be recovered from columns even under no field. There is irreversible sorption to the column packing materials. We speculate that their large magnetic moment provides a remanent magnetization at zero fields. This increases their interactions with the residual stray magnetic fields present in the column. In contrast, the smaller particles can be completely recovered at zero fields. All adsorption isotherm data were represented by the Langmuir isotherm equation, $q = bq^{\max} C/(1+bC)$, where b is the sorption constant (L/μmol) and $q^{\max}$ is the maximum sorption density of the solid (μmol/g). Fig. 4 shows an increase in the weight-based As(V) adsorption density with decreasing the particle size of Fe_3O_4. These observations result from a higher surface area due to the smaller particle size. The surface-based As(V) adsorption densities were very similar for 20 and 300 nm Fe_3O_4 nanoparticles; however, the adsorption density for 12 nm Fe_3O_4 nanoparticles was significantly increased. This observation may be attributed to more sites exposed to As adsorption, since the 12 nm Fe_3O_4 was dispersed in solution, while the 20 and 300 nm Fe_3O_4 nanoparticles were aggregated. Similar phenomenon was observed for As(III). In the desorption studies, no loss of Fe_3O_4 nanoparticles was assumed. The data in Fig. 5 illustrate the irreversible desorption of both As(III) and As(V) from 20 nm Fe_3O_4 nanoparticles. For example, approximately 1% of the adsorbed As(III) and As(V) was desorbed at pH 6.1. Similar desorption hysteresis was observed at pH 4.8 and 8.0. The high adsorption capacity and strong desorption hysteresis suggest that Fe_3O_4 nanoparticles can be useful in water treatment and solid waste disposal. In Table 1, As removal efficiency was compared assuming a treatment of 2 L of 500 μg/L As solution with 1 kg Fe_3O_4. The As removal efficiency was calculated based on Freundlich isotherm equation, $q = K_F C^N$, in the adsorption data over the range of 0–500 μg/L aqueous concentration. Decrease in residual As concentrations and increase in As removal efficiency were observed with smaller Fe_3O_4 nanoparticles. For example, with the 12 nm Fe_3O_4 nanoparticles, residual As concentrations were less than 10 μg/L and over 98% of As(III) and As(V) was removed. Our studies show that laboratory-synthesized 12 nm Fe_3O_4 nanoparticles have high As adsorption capacities. A full treatment of the sorption and desorption kinetics regarding the size dependence of Fe_3O_4 nanoparticles has been published elsewhere [12].

4. Conclusions

As removal efficiency depends strongly on the size of Fe_3O_4 sorbents. The laboratory-prepared Fe_3O_4 was not only more efficient in the removal of As, but also more easily recovered from the column of the magnetic separator than the commercial materials. This would be beneficial in a water treatment system because the As-contaminated Fe_3O_4 could be flushed from the column permitting reuse of the separator system.

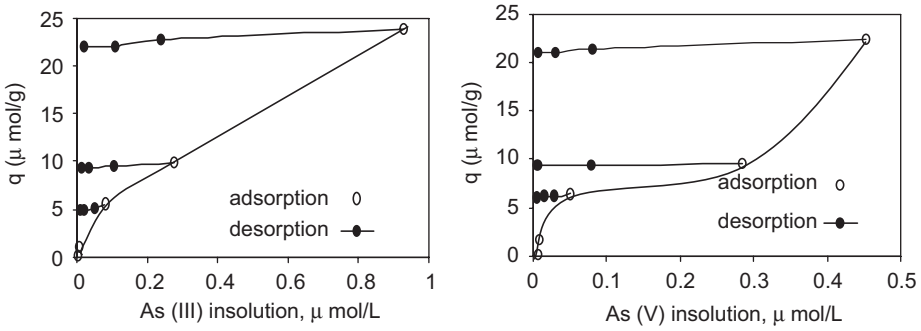

Fig. 5. Adsorption and desorption of As(III) and As(V) to 20 nm Fe_3O_4 at pH 6.1. All data were plotted as equilibrium adsorbed arsenic versus equilibrium arsenic in solution. In the desorption studies, no loss of magnetite nanoparticles was assumed.

Table 1
The effect of Fe_3O_4 size on arsenic removal efficiency

Particle size (nm)	As(V) or As(III)	Initial As concentration (μg/L)	Residual As concentration (μg/L)	% removal
12	As(III)	500	3.9	99.2
20	As(III)	500	46.3	90.9
300	As(III)	500	375.0	24.9
12	As(V)	500	7.8	98.4
20	As(V)	500	17.2	96.5
300	As(V)	500	356.4	29.2

Arsenic removal efficiency was compared assuming a treatment of 2 L of 500 μg/L arsenic solution with 1 kg magnetite. The arsenic removal efficiency was calculated using Freundlich isotherm equation, $q = K_F C^N$, in the adsorption data over the range of 0–500 μg/L aqueous concentrations.

Acknowledgment

This work was supported by the National Science Foundation through the Center for Biological and Environmental Nanotechnology at Rice University (EEC-0118007), and the Robert A. Welch Foundation (C-1349).

References

[1] M. Bissen, F.H. Frimmel, Acta Hydrochim. Hydrobiol. 31 (2003) 9.
[2] L.G. Twidwell, J. McCloskey, P. Miranda, M. Gale, in: I. Gaballah, J. Hager, R. Solozabal, (Eds.), Proceedings of the Global Symposium on Recycling, Waste Treatment and Clean Technology, Warreandale, PA, 1999, p. 1715.
[3] M.A. Hossain, et al., Environ. Sci. Technol. 39 (2005) 4300.
[4] K.P. Raven, A. Jain, R.H. Loeppert, Environ. Sci. Technol. 32 (1998) 344.
[5] M.L. Pierce, C.B. Moore, Water Res. 16 (1982) 1247.
[6] S. Fendorf, M.J. Eick, P. Grossl, D.L. Sparks, Environ. Sci. Technol. 31 (1997) 315.
[7] A. Manceau, Geochim. Cosmochim. Acta 59 (1995) 3647.
[8] G.A. Waychunas, B.A. Rea, C.C. Fuller, J.A. Davis, Geochim. Cosmochim. Acta 57 (1993) 2251.
[9] S.R. Kanel, B. Manning, L. Charlet, H. Choi, Environ. Sci. Technol. 39 (2005) 1291.
[10] S. Bucak, D.A. Jones, P.E. Laibinis, T.A. Hatton, Biotechnol. Prog. 19 (2003) 477.
[11] G.D. Moeser, K.A. Roach, W.H. Green, P.E. Laibinis, T.A. Hatton, Ind. Eng. Chem. Res. 41 (2002) 4739.
[12] S. Yean, et al., J. Mater. Res. 20 (2005) 3255.
[13] W.W. Yu, J.C. Falkner, C.T. Yavuz, V.L. Colvin, Chem. Commun. (2004) 2306.
[14] L.P. Ramirez, K. Landfester, Chem. Phys. 204 (2003) 22.